

Electrochemical Nickel-Catalyzed C(sp²)-H Functionalization of Tropones with Aldehydes

Andrea Brunetti, Sofia Kiriakidi, Mauro Garbini, Giulia Monda, Chiara Zanardi, Carlos Silva López,* Giulio Bertuzzi,* and Marco Bandini*



Cite This: *ACS Catal.* 2025, 15, 3184–3190



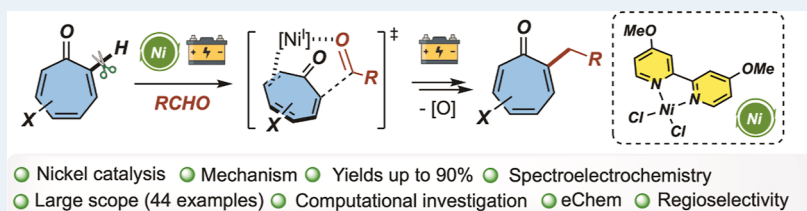
Read Online

ACCESS |

Metrics & More

Article Recommendations

Supporting Information



ABSTRACT: A direct electroreductive functionalization of tropones employing aldehydes as alkylating agents is reported. This C(sp²)-H functionalization process leverages the mediation of electroactive nickel complexes, enabling a wide range of both native and substituted tropones (44 examples) to be alkylated selectively at the α -position in high yields (up to 90%). Combined electrochemical, spectroelectrochemical, and computational analyses disclosed the whole mechanistic pathway and revealed the key role played by reduced Ni complexes in activating the troponone core toward condensation with the aldehydes.

KEYWORDS: electrocatalysis, nickel-catalysis, tropones, aldehydes, DFT calculations, cyclovoltammetry

INTRODUCTION

Troponone and tropolone derivatives are widely distributed in naturally occurring compounds and bioactive ingredients.¹ Colchicine, purpurogallin, harringtonolide, and roseobacticide B are representative examples of densely polycyclic scaffolds that include the cycloheptatrienone scaffold (Figure 1a).² Not surprisingly, attention to troponone synthetic chemistry grew rapidly leading to the publication of elegant total syntheses of troponone-based bioactive compounds.

However, from a synthetic viewpoint, the peculiar seven-membered structure combined with its nonbenzenoid aromaticity appoints troponone as nontrivial platforms to generate chemical complexity. As such, they call for innovative synthetic organic transformations.

Nowadays, the existing portfolio of troponone chemistry primarily focuses on dearomative cycloaddition reactions³ or the de novo assembly of the 7-membered ring.⁴ Conversely, investigations into chemical troponone decorations, via direct C–H functionalization, still remains largely elusive.⁵ Impracticability of Friedel–Crafts-type transformations (troponone features an overall electron-poor aromatic core); atypical reactivity of the formal C=O unit (troponone is better represented as tropylium oxide), and high propensity toward dearomatization processes represent the most stringent traits that still narrow this scenario (Figure 1b).

To overcome these issues, we propose a new functionalization strategy built upon considering a chemical conceptual analogy between α,β -unsaturated carbonyls (i.e., cyclohexanone or

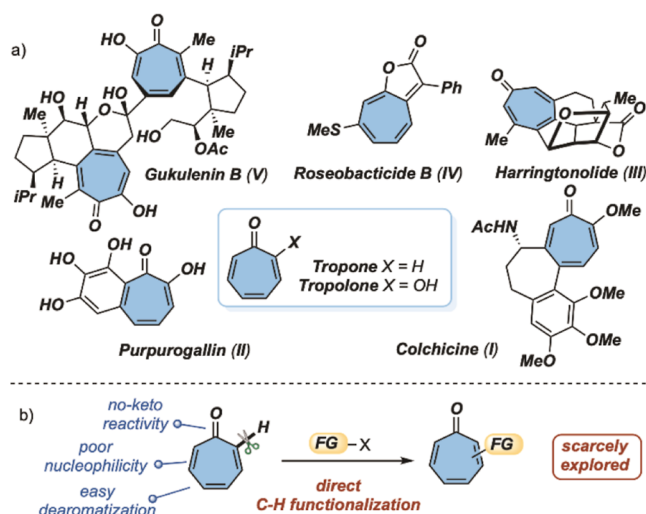


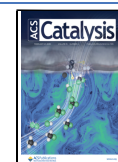
Figure 1. (a) Troponone derivatives: ubiquitous platforms for bioactive structures. (b) Main shortcomings that still limit the functionalization of troponone via C–H functionalization.

Received: November 19, 2024

Revised: January 10, 2025

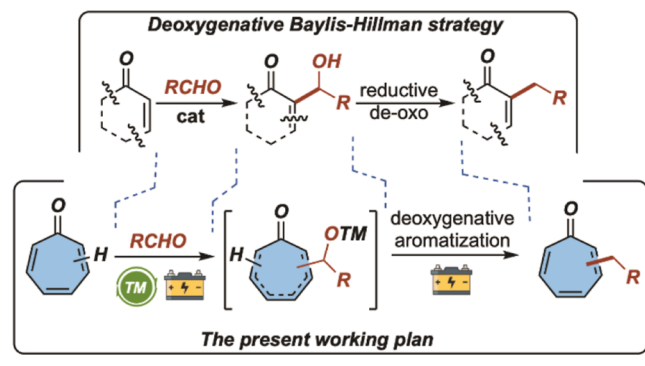
Accepted: January 13, 2025

Published: February 7, 2025



methyl acrylate) and tropones, with a focus on the well-established deoxygenative Baylis–Hillman strategy (Scheme 1-up), where after the (redox-neutral) Baylis–Hillman reaction has taken place, a following distinct reductive deoxygenation step is carried out.⁶

Scheme 1. Present Electrochemical Strategy for the Direct Access of C–H Functionalization of Tropones Gets Inspired by the Deoxygenative BH Reaction



In particular, we hypothesized that direct C–C bond formation on the seven-membered ring could be achieved under reductive electrochemical conditions using aldehydes as convenient alkylating agents⁷ and low-oxidation state transition metals (TMs) to trigger a cross-electrophile-coupling-like strategy.⁸ In addition, the formation of metal-alkoxide intermediates could facilitate the *situ* final deoxygenation stage without the need for exogenous stoichiometric reducing agents (Scheme 1-bottom).

The feasibility of this working plan is strongly substantiated by our recent experience in proving electroreductive cross-electrophile couplings as an excellent enabling technology for the efficient functionalization of both Morita-Baylis–Hillman⁹ and tropones derivatives.¹⁰

METHODS

In particular, due to the well-established efficiency of nickel complexes in mediating electrocatalytic organic transformations,¹¹ we preliminarily targeted readily available and air-stable bispyridil-Ni(II) complexes [Ni(L)Cl₂] in the presence of 2-phenyl-troponone **1a** and *p*-Cl-benzaldehyde **2a** as model substrates. Remarkably, the presence of a catalytic amount of a nickel complex (15 mol %) proved essential to guarantee synthetically useful conversions (entry 1 vs entries 2–5). In detail, by means of the sacrificial anode strategy (Zn), isolated yields up to 83% on the site-selective α -alkylation of **1a** were recorded (entry 2, Table 1). Here, 4,4'-(OMe)₂-bpy (L1) appeared as the ligand of selection among those tested (L1–4). Moreover, from the electrode-couple screening, it is worth mentioning that a metal cathode and a Zn anode are essential to get a productive outcome, with the Ni(–)/Zn(+) couple proving superior with respect to all other combinations tested (i.e., W/Zn, C/Zn, SS/Zn, and Ni/Mg, entry 2 vs entries 6–9).

Additionally, optimal reaction conditions involved constant current electrolysis (CCE, *I* = 2 mA) providing 4 F/mol with reference to the limiting reagent **2a**, stoichiometrically necessary to react all reagent **1a** (entries 2 vs entries 10 and 11), and using tetraethylammonium tetrafluoroborate (TEABF₄) as the electrolyte (entries 2 vs entries 12 and 13).

Table 1. Optimization of the Reaction Conditions^a

run	L	electrolysis conditions	yield 3aa (%) ^b
1	^c	Ni/Zn, 2 mA, 4 F/mol, TEABF ₄	15
2	L1	Ni/Zn, 2 mA, 4 F/mol, TEABF ₄	83
3	L2	Ni/Zn, 2 mA, 4 F/mol, TEABF ₄	39
4	L3	Ni/Zn, 2 mA, 4 F/mol, TEABF ₄	65
5	L4	Ni/Zn, 2 mA, 4 F/mol, TEABF ₄	60
6	L1	W/Zn, 2 mA, 4 F/mol, TEABF ₄	75
7	L1	SS/Zn, 2 mA, 4 F/mol, TEABF ₄	54
8	L1	C/Zn, 2 mA, 4 F/mol, TEABF ₄	NR
9	L1	Ni/Mg, 2 mA, 4 F/mol, TEABF ₄	traces ^d
10	L1	Ni/Zn, 3 mA, 4 F/mol, TEABF ₄	26
11	L1	Ni/Zn, 1.5 mA, 4 F/mol, TEABF ₄	41
12	L1	Ni/Zn, 2 mA, 4 F/mol, LiBF ₄	24
13	L1	Ni/Zn, 2 mA, 4 F/mol, TEACl	<10

^aAll reactions were carried out in an ElectraSyn 2.0 apparatus by means of undivided cell strategy at room temperature. Anhydrous conditions and inert atmosphere (i.e. N₂) were applied. **1a**/**2a**/electrolyte = 2:1:1.5, [**2a**]: 0.05 M. ^bIsolated yield after flash chromatography. ^cIn absence of Ni-catalyst. ^dExtensive decomposition of **1a** was observed in the reaction crude. NR: no reaction.

The generality of the present electrochemical procedure was then assessed by subjecting a range of α -substituted tropones (**1b–s**) as well as native troponone **1t** to reductive alkylating conditions with a family of aldehydes **2b–s** (aromatic as well as aliphatic). The obtained results are summarized in Scheme 2.

Aromatic aldehydes (**2b–n**) proved competent as benzylating agents regardless of the nature of the substituents and their positions (Scheme 2 upper). In particular, strong as well as mild electron-withdrawing groups (EWGs: F, CF₃, and Cl) could be accommodated at ortho-, meta-, and para-positions, ensuring satisfying levels of chemical outcomes (yield up to 77%). Analogously, aldehydes carrying electron-donating units (EDGs: alkyl, phenyl, and OMe) on the aromatic ring and benzofused carbonyls (**2c,d**) underwent the α -benzylation of 2-phenyltroponone **1a** in synthetically useful yields (44–81%). Interestingly, the alkylation methodology could also be extended to aliphatic aldehydes (**2o,s**). In this regard, linear and branched alkyl chains could be conveniently introduced in the seven-membered ring unit via direct activation of the C(sp²)-H bond (yield up to 52%). A range of α -aryltropones was also compatible with this protocol (**1b–r**, Scheme 2 center), allowing combinations of substituted α -aryl and α -benzyl units without affecting the corresponding C–H functionalization/alkylation process. Notably, a wide range of functional groups (e.g., TMS, Ac, and CN) and heteroaromatic arenes were tolerated under these conditions, yielding the desired compounds **3** in moderate to very high yields (up to 83%). An excursion away from the starting aromatics also showed that α -acetamide groups are compatible with this approach (**3sb**).

Although α -substituted tropones were initially targeted aiming to exploit the higher stability of the corresponding alkylated compounds, we then turned our attention toward the

Scheme 2. Scope of the Reaction. Upper: Screening of Different Aldehydes (1b-s) as Alkylating Agents. Center: Screening of Diversely α -substituted Tropones. Lower: Testing the Unsubstituted Troponone **1t under Optimal Mono- and di-alkylating Electrochemical Conditions. All Reactions Were Carried out under Optimal Conditions Described in Table 1, Entry 2**

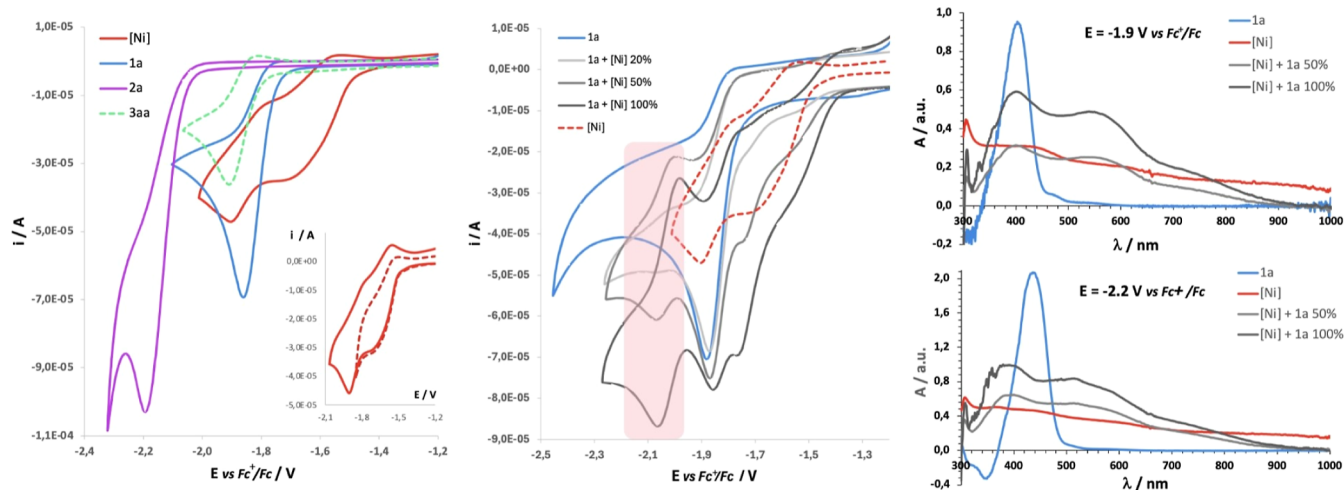
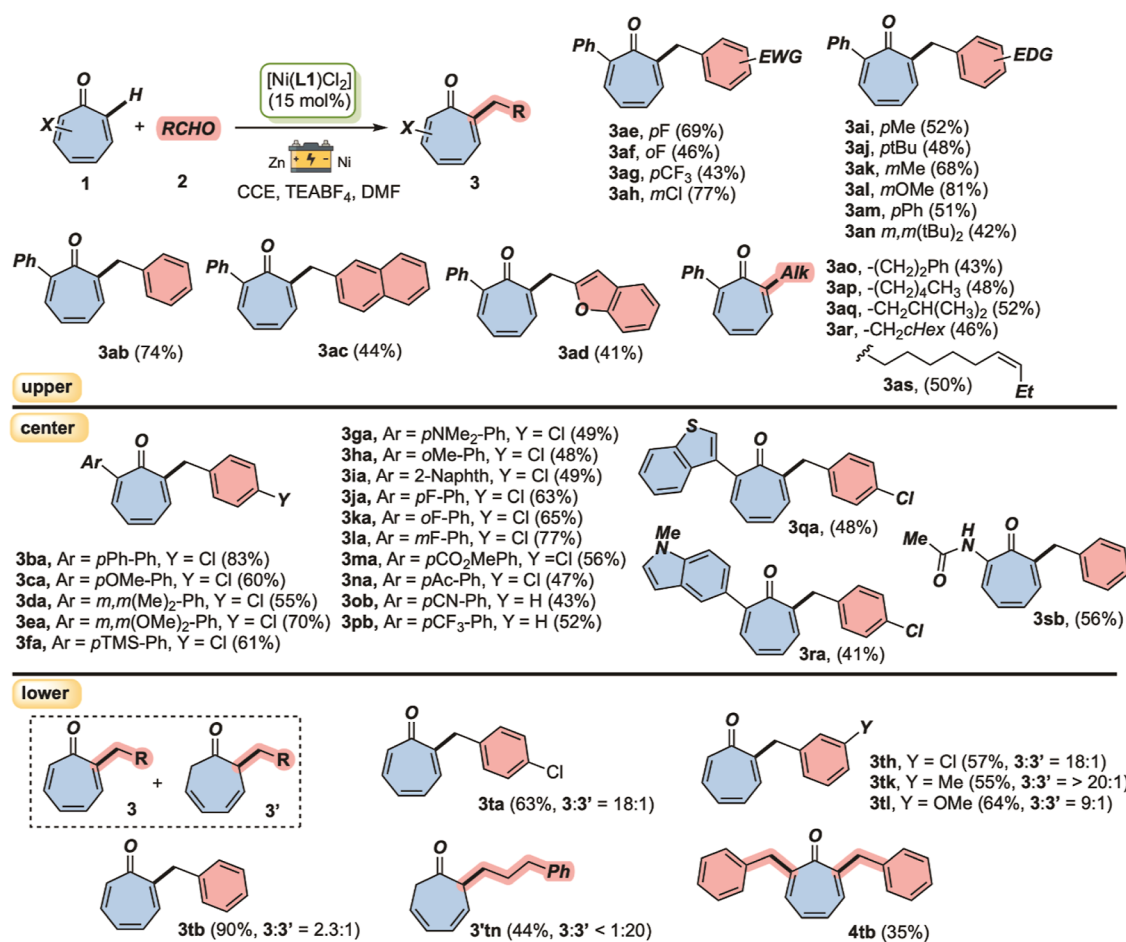


Figure 2. CV responses of (a) various species participating in the electrochemical reaction (inset highlights the two reduction processes of [Ni]) and (b) for subsequent addition of [Ni] in a solution containing a fixed amount of **1a** (pink bar highlights the new reversible reduction process ascribable to the intermediate of the reaction). Figure also reports UV-vis spectra recorded in the various solutions during the polarization of the electrode at (c) -1.9 V and (d) -2.2 V vs Fc^+/Fc .

more challenging native troponone **1t** as a platform for the benzylation protocol (Scheme 2 lower).

Satisfyingly, the electrochemical α -alkylation of the unsubstituted troponone was found to be highly efficient with a range of

both aromatic and aliphatic aldehydes. In particular, combined chemical yields up to 90% (including partially reduced cycloheptadienones **3'**) were recorded. The use of troponone **1t** also inspired us to challenge our protocol with a one-pot double

alkylation strategy. Interestingly, by using an excess of benzaldehyde (**2b**), the 2,7-dibenzylated tropone **4tb** was isolated in an unoptimized yield (35%).

In order to initiate the investigation of the reaction mechanism, cyclic voltammetric analyses were first conducted on the various reaction components. As observed from the voltammetric responses collected (3-electrode cell, Figure 2a), the $[\text{Ni}(\text{L1})\text{Cl}_2]$ complex ($[\text{Ni}]$) shows two reduction processes, the first occurring at -1.75 V vs the Fc^+/Fc redox couple, and the second one at -1.90 V. Therefore, the first reduction of this complex occurs at lower potentials with respect to the process involving both **1a** (-1.87 V) and **2a** (-2.18 V), suggesting that the catalytic cycle is initiated by a monoelectronic reduction of the starting Ni(II) complex to furnish a Ni(I) intermediate.

Then, to get further details about the initial stages of the reaction machinery, we conducted additional voltammetric experiments of the $[\text{Ni}]-\mathbf{1a}$ mixture, by systematically increasing the concentration of $[\text{Ni}]$ in a solution at a fixed concentration of **1a** (Figure 2b).¹² A new peak appearing in the voltammograms of these mixtures suggests the formation of a new species showing a reversible reduction with $E_{1/2} = -1.98$ V vs Fc^+/Fc (see the pink area in Figure 2b).

This could be ascribed to a $[\text{Ni}]-\mathbf{1a}$ intermediate being formed during the electrochemical reaction, increasing in intensity along with an increasing concentration of $[\text{Ni}]$. This new species is reduced at a more negative potential than the starting complex $[\text{Ni}]$ and also at a different potential than that expected for the free **L1** (-2.72 V), allowing for its observation by CV analyses. A similar electrochemical process was also observed by adding **1a** to a solution containing a fixed concentration of $[\text{Ni}]$ (see Figure S1). This new electroactive organo-nickel intermediate was therefore postulated as a key for the formation of **3aa** upon reaction with **2a** (vide infra on mechanistic investigation). To corroborate this hypothesis, we recorded UV-vis spectra of solutions containing either **1a**, $[\text{Ni}]$ or mixtures of the two species while polarizing a Pt grid working electrode (spectra recorded at the various potentials are reported in Figure S2). Interestingly, spectra recorded right before (-1.90 V, Figure 2c) and after (-2.20 V, Figure 2d) the reversible reduction peak associated with the $[\text{Ni}]-\mathbf{1a}$ intermediate,¹³ evidenced that this new species exhibits a main absorption at 560 nm in the neutral form (-1.90 V), or one at 520 nm after being reduced (-2.20 V). Furthermore, the lower intensity of the adsorption recorded at 400 nm (i.e., reduction of **1a**) when analyzing the mixture suggests that the starting tropone is involved in the reaction with $[\text{Ni}]$. Through computational exploration (vide infra), we have found a $[\text{Ni}]$ complex whose simulated UV-vis absorption bands in the oxidation state Ni(I) correlate well with those found in these experiments (Figure S3-top). As a result, we have collected experimental and computational indications that in the initial stages of the reaction, Ni(II) is reduced to Ni(I), which subsequently reacts to form a complex with **1a**, resulting in an organo-nickel intermediate.

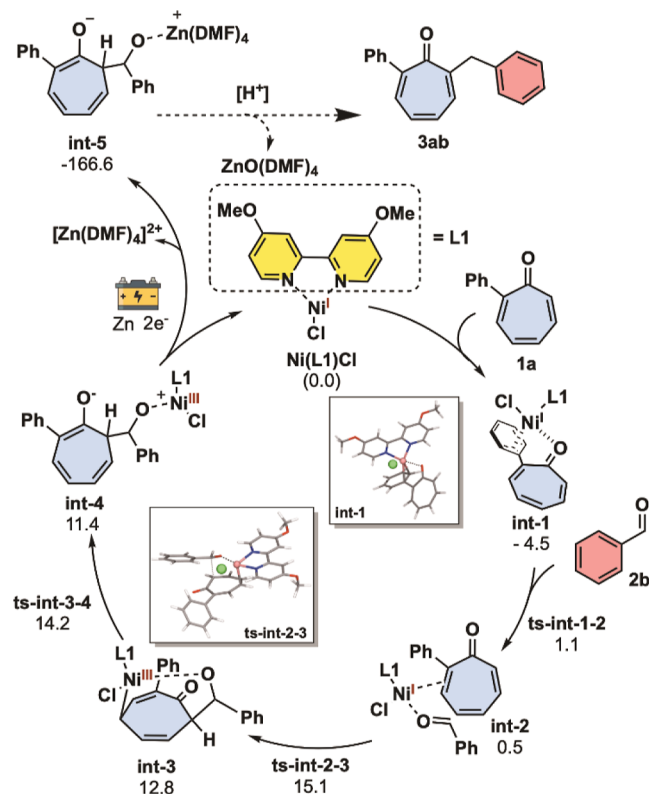
These intriguing results prompted us to perform a computational investigation to gain further insights into the underlying mechanism and the nature of the organo-nickel species involved. We employed density functional theory (DFT) calculations conducted at the SMD¹⁴ (DMF) M06¹⁵/def2svp(p)¹⁶ level of theory, using the Gaussian 09 software¹⁷ (see the Supporting Information for the full computational protocol). The results of

the electrochemical tests suggested a reaction initiated by the Ni(I) species.

To elucidate the identity of the Ni species, we calculated UV-vis spectra for the $[\text{Ni}(\text{I})(\text{L1})\text{Cl}]$ catalyst and compared them with the experimental spectra shown in Figure 2. The calculated absorption peaks for $[\text{Ni}(\text{I})]$ at 376 and 442 nm (Figure S3, top) closely align with the experimental values of 365 and 440 nm. Then, we next investigated the formation of a $[\text{Ni}]-\mathbf{1a}$ species, as suggested by the spectro-electrochemical investigation. Here, our calculations showed that a π -O-chelated organonickel complex **int-1** is formed in a barrierless exothermic process, stabilized by 4.5 kcal/mol. **Int-1** has a chelating-like coordination mode of the Ni(I) metal center with **1a** through contacts involving the π -electron cloud of the phenyl ring (η^2 -like hapticity) and the lone pair of the oxygen atom of the tropone core. The computational spectra showed a good agreement with the experimental ones (Figure S3, bottom) with absorption peaks at 430, 572, 604, and 607 nm.

In the next step, the Ni-center (**int-2**, Scheme 3) is proposed to act as a tethering unit to bring in proximity benzaldehyde **2b**

Scheme 3. Suggested Reaction Mechanism Computed at the DFT (M06/def2svp(p)) Level of Theory. The Energies Are Reported in Kcal/mol and Correspond to Relative ΔG (Reported Below Minima Structures) and ΔG^{\ddagger} (Reported Next/below Arrows)



(weak Ni–O coordination) and tropone **1a** (interacting with the ε - ζ double bond). This coordination results in a net transfer of electron-density from the metal center to the tropone as supported by the electrostatic potential and the NBO charges computed on **int-2** and **int-3** (Figure S5). In particular, upon nickel coordination (**int-2**), the tropone unit carries a negative charge of -0.43 au, while the aldehyde is unperturbed ($+0.06$ a.u.). This interaction leads to an overall umpolung of reactivity

of the tropone and triggers the consequent nucleophilic condensation to the aldehyde (**ts-int-2-3**: 15.1 kcal/mol).^{18,19} The consequent C–C bond formation event occurs exclusively at the α -carbon of tropone, leading to the organo-Ni(III) **int-3** eventually featuring a C(δ)-Ni bond. Next, the weak Ni–C bond is broken with an activation energy of only 1.4 kcal/mol and a new Ni(III)–O alkoxide **int-4** is obtained.

At this point, the final electrochemical reduction of Ni(III) to Ni(I) restores the catalytically active species and a Zn–Ni ion-exchange, between **int-3** and the Zn(II) ions liberated from the sacrificial anode,²² affords the zinc-alkoxide **int-5** through a strongly exothermic step. This last intermediate is ready to furnish the final product either directly or assisted by the mild acidic media used during the work-up process.

Finally, due to the well-known propensity of organonickel species to react via single-electron-transfer (SET) processes,^{20,21} we investigated the possibility of a SET event occurring in our case, by using Marcus Theory²³ and the methodology described in the reference (Figure S4).²⁴ Interestingly, the single-electron-transfer alternative that would turn **1a** into a nucleophilic species, able to trap the electrophilic aldehyde, proved unlikely as it requires an activation energy of 30.9 kcal/mol for the initial step: $\mathbf{1a} + [\text{Ni(I)}] \rightarrow [\mathbf{1a}]^{-\bullet} + [\text{Ni(II)}]^+$.

CONCLUSIONS

In conclusion, the combined use of nickel catalysis and electrosynthesis has been documented as an efficient strategy to accomplish a general α -alkylation of tropones via C–H functionalization. The present cross-electrophile coupling involves common aldehydes as alkylating agents. A dedicated spectro-electrochemical study sheds light on the active role of the nickel complex in the redox process. Here, the tropone core proved to be an effective π -ligand (acceptor) for the Ni-center, prompting an umpolung of reactivity of the seven-member ring. Finally, all of the catalytic mechanism was computed at the DFT level of theory, relying on close agreements with both experimental and spectroscopic analyses. In particular, the respective behavior of the two electrophiles (tropone and aldehyde) in the present cross-coupling as well as the nature of the catalytically active Ni-species have been elucidated.

ASSOCIATED CONTENT

Supporting Information

The Supporting Information is available free of charge at <https://pubs.acs.org/doi/10.1021/acscatal.4c07120>.

Experimental procedures, characterization data, and additional optimization data (PDF)

AUTHOR INFORMATION

Corresponding Authors

Carlos Silva López – *Departamento de Química Orgánica, Universidade de Vigo, Vigo 36310, Spain;*
Email: carlos.silva@uvigo.gal

Giulio Bertuzzi – *Dipartimento di Chimica “Giacomo Ciamician”, Alma Mater Studiorum – Università di Bologna, Bologna 40129, Italy; Center for Chemical Catalysis – C3, Alma Mater Studiorum – Università di Bologna, Bologna 40129, Italy; Email: giulio.bertuzzi2@unibo.it*

Marco Bandini – *Dipartimento di Chimica “Giacomo Ciamician”, Alma Mater Studiorum – Università di Bologna, Bologna 40129, Italy; Center for Chemical Catalysis – C3, Alma Mater Studiorum – Università di Bologna, Bologna 40129, Italy; orcid.org/0000-0001-9586-3295;*
Email: marco.bandini@unibo.it

40129, Italy; orcid.org/0000-0001-9586-3295;

Email: marco.bandini@unibo.it

Authors

Andrea Brunetti – *Dipartimento di Chimica “Giacomo Ciamician”, Alma Mater Studiorum – Università di Bologna, Bologna 40129, Italy; Center for Chemical Catalysis – C3, Alma Mater Studiorum – Università di Bologna, Bologna 40129, Italy*

Sofia Kiriakidi – *Dipartimento di Chimica “Giacomo Ciamician”, Alma Mater Studiorum – Università di Bologna, Bologna 40129, Italy; Departamento de Química Orgánica, Universidade de Vigo, Vigo 36310, Spain*

Mauro Garbini – *Dipartimento di Chimica “Giacomo Ciamician”, Alma Mater Studiorum – Università di Bologna, Bologna 40129, Italy; Center for Chemical Catalysis – C3, Alma Mater Studiorum – Università di Bologna, Bologna 40129, Italy*

Giulia Monda – *Dipartimento di Chimica “Giacomo Ciamician”, Alma Mater Studiorum – Università di Bologna, Bologna 40129, Italy; Center for Chemical Catalysis – C3, Alma Mater Studiorum – Università di Bologna, Bologna 40129, Italy*

Chiara Zanardi – *Department of Molecular Sciences and Nanosystems, Ca’ Foscari University of Venice, Venezia (Mestre) 30170, Italy; Institute for Organic Synthesis and Photoreactivity (ISOF), National Research Council of Italy (CNR), Bologna 40129, Italy; orcid.org/0000-0002-2091-3398*

Complete contact information is available at:

<https://pubs.acs.org/10.1021/acscatal.4c07120>

Author Contributions

The manuscript was written through contributions of all authors. All authors have given approval to the final version of the manuscript.

Notes

The authors declare no competing financial interest.

ACKNOWLEDGMENTS

We are grateful to the University of Bologna for financial support and PRIN-2022-PNRR project (20227Z3BL8). M.B. is also grateful to Consorzio CINMPIS. S.K. thanks the Xunta de Galicia for funding through the fellowship “Ayudas de apoyo a la etapa de formación posdoctoral (ED481B-2023-044)”. CSL is grateful to the Centro de Supercomputación de Galicia for HPC resources and to MICINN (PID2020-115789G.B.-C22) for research funds. C.Z. is grateful to the group of Prof. Erika Scavetta (University of Bologna) for the use of the spectrophotometric equipment.

ABBREVIATIONS

BH, Baylis–Hillman; CCE, constant current electrolysis; DFT, density functional theory; EDG, electron-donating; EWG, electron-withdrawing; NBO, natural bond orbital; SET, single-electron transfer; SS, stainless steel; TEABF₄, tetraethylammonium tetrafluoroborate; TM, transition metal.

REFERENCES

- (1) (a) Bentley, R. A Fresh Look at Natural Tropoloneoids. *Nat. Prod. Synth.* **2008**, *25*, 118–138. (b) Guo, H.; Roman, D.; Beemelmans, C. Tropolone Natural Products. *Nat. Prod. Rep.* **2019**, *36*, 1137–1155. (c) Höing, L.; Sowa, S. T.; Toplak, M.; Reinhardt, J. K.; Jakob, R.;

Maier, T.; Lill, M. A.; Teufel, R. Biosynthesis of the Bacterial Antibiotic 3,7-Dihydroxytropolone Through enzymatic Salvaging of Catabolic Shunt Products. *Chem. Sci.* **2024**, *15*, 7749–7756.

(2) For selected examples on total synthesis of tropone-containing bioactive compounds see: (a) Graening, T.; Schmalz, H.-G. Total Syntheses of Colchicine in Comparison: A Journey through 50 Years of Synthetic Organic Chemistry. *Angew. Chem., Int. Ed.* **2004**, *43*, 3230–3256. (b) Williams, R. V.; Edwards, W. D.; Zhang, P.; Berg, D. J.; Mitchell, R. H. Experimental Verification of the Homoaromaticity of 1,3,5-Cycloheptatriene and Evaluation of the Aromaticity of Tropone and the Tropylium Cation by Use of the Dimethyldihydropyrene Probe. *J. Am. Chem. Soc.* **2012**, *134*, 16742–16752. (c) Kats-Kagan, R.; Herzog, S. B. The Discovery of a Novel Route to Highly Substituted α -Tropolones Enables Expedient Entry to the Core of the Gukulenins. *Org. Lett.* **2015**, *17*, 2030–2033. (d) Nicolaou, K. C.; Yu, R.; Lu, Z.; Alvarez, F. G. Total Synthesis of Gukulenin B via Sequential Tropolone Functionalizations. *J. Am. Chem. Soc.* **2022**, *144*, 5190–5196. (e) Sun, Z.; Shu, X.; Ma, F.; Li, A.; Li, Y.; Jin, S.; Wang, Y.; Hu, X. Divergent Synthesis of 17-nor-Cephalotane Diterpenoids through Developed Ynol-diene Cyclization. *Angew. Chem., Int. Ed.* **2024**, *63*, No. e202407757. (f) Wiesler, S.; Sennari, G.; Popescu, M. V.; Gardner, K. E.; Aida, K.; Paton, R. S.; Sarpong, R. Late-stage Benzenoid-to-troponoid Skeletal Modification of the Cephalotanes Exemplified by the Total Synthesis of Harringtonolide. *Nat. Commun.* **2024**, *15*, 4125.

(3) (a) Jessen, N. I.; McLeod, D.; Jørgensen, K. A. Higher-Order Cycloaddition Reactions for the Construction of Polycyclic Aromatic and Polycyclic Heteroaromatic Compounds. *Chemistry* **2022**, *8*, 20–30. (b) Domingo, L. R.; Pérez, P. Understanding the Higher-order Cycloaddition Reactions of Heptafulvene, Tropone, and its Nitrogen Derivatives, with Electrophilic and Nucleophilic Ethylenes Inside the Molecular Electron Density Theory. *New J. Chem.* **2022**, *46*, 11520–11530. (c) Pradhan, P.; Das, I.; Debnath, S.; Parveen, S.; Das, T. Synthesis of Substituted Tropones and Advancement for the Construction of Structurally Significant Skeletons. *ChemistrySelect* **2022**, *7*, No. e202200440. (d) Garcia, M. R.; Iribarren, I.; Rozas, I.; Trujillo, C. Simultaneous Hydrogen Bonds with Different Binding Modes: The Acceptor “Rules” but the Donor “Chooses.” *Chem.—Eur. J.* **2023**, *29*, No. e202301223. (e) Murelli, R. P.; Berkowitz, A. J.; Zuschlag, D. W. Carbocycloaddition Strategies for Tropenoid Synthesis. *Tetrahedron* **2023**, *130*, 133175. (f) Zheng, T.; Zikuan, N.; Mitschke, B.; List, B. A Solid noncovalent Organic Double-Helix Framework Catalyzes Asymmetric [6 + 4] Cycloaddition. *Science* **2024**, *385*, 765–770. (g) Zhang, B.; Wang, J. Recent Advances on Metal-free Catalytic Enantioselective Higher-Order Cycloadditions. *Org. Chem. Front.* **2024**, *11*, 1824–1842.

(4) Liu, N.; Song, W.; Schienebeck, C. M.; Zhang, M.; Tang, W. Synthesis of Naturally Occurring Tropones and Tropolones. *Tetrahedron* **2014**, *70*, 9281–9305.

(5) (a) Haas, D.; Sustac-Roman, D.; Schwarz, S.; Knochel, P. Directed Zincation with $\text{TMPZnCl}\cdot\text{LiCl}$ and Further Functionalization of the Tropolone Scaffold. *Org. Lett.* **2016**, *18*, 6380–6383. (b) Jena, C. K.; Sharma, N. K. Novel Cinnamic Acid Analogues: Synthesis of Aminotroponyl Acrylates by Pd(II)-catalysed $\text{C}(\text{sp}^2)\text{—H}$ Olefination. *Chem. Commun.* **2022**, *58*, 8077–8080.

(6) (a) Ullah, H.; Ferreira, A. V.; Bendassolli, J. A.; Rodrigues, M. T.; Formiga, A. L. B.; Coelho, F. A Versatile Approach to Noncoded β -Hydroxy- α -amino Esters and α -Amino Acids/Esters from Morita–Baylis–Hillman Adducts. *Synthesis* **2014**, *47*, 113–123. (b) Narayanan, D.; Tran, K. T.; Pallesen, J. S.; Solbak, S. M. O.; Qin, Y.; Mukminova, E.; Luchini, M.; Vasilyeva, K. O.; González Chichón, D.; Goutsiou, G.; Poulsen, C.; Haapanen, N.; Popowicz, G. M.; Sattler, M.; Olganier, D.; Gajhede, M.; Bach, A. Development of Noncovalent Small-Molecule Keap1-Nrf2 Inhibitors by Fragment-Based Drug Discovery. *J. Med. Chem.* **2022**, *65*, 14481–14526.

(7) Wang, Y.; Wu, Q.-Q.; Tian, S.-K. Advances in Organic Reactions. *J. Org. Chem.* **2023**, *88*, 16456–16466.

(8) (a) Ma, C.; Fang, P.; Liu, Z.-R.; Xu, S.-S.; Xu, K.; Cheng, X.; Lei, A.; Xu, H.-C.; Zeng, C.; Mei, T.-S. Recent Advances in Organic

Electrosynthesis Employing Transition Metal Complexes as Electrocatalysts. *Sci. Bull.* **2021**, *66*, 2412–2429. (b) Qiu, Y.; Li, P. Reductive Electrophilic Cross-Coupling for Constructing $\text{C}(\text{sp}^3)\text{—C}(\text{sp}^3)$ Bonds. *Synlett* **2024**.

(9) (a) Bertuzzi, G.; Ombrosi, G.; Bandini, M. Regio- and Stereoselective Electrochemical Alkylation of Morita–Baylis–Hillman Adducts. *Org. Lett.* **2022**, *24*, 4354–4359. (b) Rapisarda, L.; Fermi, A.; Ceroni, P.; Giovannelli, R.; Bertuzzi, G.; Bandini, M. Electrochemical $\text{C}(\text{sp}^3)\text{—H}$ Functionalization of Ethers via Hydrogen-atom Transfer by Means of Cathodic Reduction. *Chem. Commun.* **2023**, *59*, 2664–2667. (c) Brunetti, A.; Bertuzzi, G.; Bandini, M. Catalyst- and Additive-Free Electrochemical CO_2 Fixation into Morita–Baylis–Hillman Acetates. *Synthesis* **2023**, *55*, 3047–3055.

(10) (a) Brunetti, A.; Garbini, M.; Gino Kub, N.; Monari, M.; Pedrazzani, R.; Zanardi, C.; Bertuzzi, G.; Bandini, M. Electrochemical Site-Selective Alkylation of Tropones via Formal $\text{C}(\text{sp}^3)\text{—C}(\text{sp}^2)$ Coupling Reaction. *Adv. Synth. Catal.* **2024**, *366*, 1965–1971. (b) For other electroreductive processes, see: Garbini, M.; Brunetti, A.; Pedrazzani, R.; Monari, M.; Marcaccio, M.; Bertuzzi, G.; Bandini, M. Reductive Cyclodimerization of Chalcones: Exploring the “Self-adaptability” of Galvanostatic Electrosynthesis. *Chem. Commun.* **2024**, *60*, 404–407. (c) Brunetti, A.; Garbini, M.; Autuori, G.; Zanardi, C.; Bertuzzi, G.; Bandini, M. Electrochemical Synthesis of Itaconic Acid Derivatives via Chemodivergent Single and Double Carboxylation of Allenes with CO_2 . *Chem.—Eur. J.* **2024**, *30*, No. e202401754.

(11) For general reviews, see: (a) Jose, J.; Diana, E. J.; Kanchana, U. S.; Mathew, T. V. Recent Advances in the Nickel-catalysed Electrochemical Coupling Reactions with a Focus on the Type of Bond Formed. *Asia J. Org. Chem.* **2023**, *12*, No. e202200593. (b) Liu, Y.; Li, P.; Wang, Y.; Qiu, Y. Electroreductive Cross-Electrophile Coupling (eXEC) Reactions. *Angew. Chem., Int. Ed.* **2023**, *62*, No. e202306679. (c) Franke, M.; Weix, D. J. Recent Advances in Electrochemical, Ni-Catalyzed C—C Bond Formation. *Isr. J. Chem.* **2024**, *64*, No. e202300089. (d) See also: Oksanen, V.; Rautiainen, S.; Wirtanen, T. Nickel-Electrocatalyzed Synthesis of Bifuran-Based Monomers. *Chem.—Eur. J.* **2023**, *29*, No. e202302572. (e) Zou, L.; Wang, X.; Xiang, S.; Zheng, W.; Lu, Q. Paired Oxidative and Reductive Catalysis: Breaking the Potential Barrier of Electrochemical $\text{C}(\text{sp}^3)\text{—H}$ Alkenylation. *Angew. Chem., Int. Ed.* **2023**, *62*, No. e202301026. (f) Reboli, M.; Kassamba, S.; Durandetti, M. Nickel-Catalyzed Intramolecular Hydrosilylation of Alkynes: Embracing Conventional and Electrochemical Routes. *Chem.—Eur. J.* **2024**, *30*, No. e202400440. (g) Luo, J.; Davenport, M. T.; Ess, D. H.; Liu, T. L. Nickel-Catalyzed Electrochemical Cross-Electrophile $\text{C}(\text{sp}^2)\text{—C}(\text{sp}^3)$ Coupling via a Ni^{II} Aryl Amido Intermediate. *Angew. Chem., Int. Ed.* **2024**, *63*, No. e202407118. (h) Chen, M.-Y.; Charvet, S.; Payard, P.-A.; Perrin, M.-E. L.; Vantourout, J. C. Electrochemically Driven Nickel-Catalyzed Halogenation of Unsaturated Halide and Triflate Derivatives. *Angew. Chem., Int. Ed.* **2024**, *63*, No. e202311165.

(12) The voltammograms of the $[\text{Ni}]\text{-1a}$ mixtures become more complex but still contain the signatures of the components.

(13) At these potentials, the initial $[\text{Ni}]\text{-1a}$ species is considered to be in the neutral and reduced states.

(14) Marenich, A. V.; Cramer, C. J.; Truhlar, D. G. Universal Solvation Model Based on Solute Electron Density and on a Continuum Model of the Solvent Defined by the Bulk Dielectric Constant and Atomic Surface Tensions. *J. Phys. Chem. B* **2009**, *113*, 6378–6396.

(15) (a) Zhao, Y.; Truhlar, D. G. The M06 Suite of Density Functionals for Main Group Thermochemistry, Thermochemical Kinetics, Noncovalent Interactions, Excited States, and Transition Elements: two new Functionals and Systematic Testing of four M06-class Functionals and 12 other Functionals. *Theor. Chem. Acc.* **2008**, *120*, 215–241. (b) Zhao, Y.; Truhlar, D. G. Density Functionals with Broad Applicability in Chemistry. *Acc. Chem. Res.* **2008**, *41*, 157–167.

(16) (a) Weigend, F. Accurate Coulomb-fitting Basis Sets for H to Rn. *Phys. Chem. Chem. Phys.* **2006**, *8*, 1057–1065. (b) Weigend, F.; Ahlrichs, R. Balanced Basis Sets of Split Valence, Triple Zeta Valence

and Quadruple Zeta Valence Quality for H to Rn: Design and Assessment of Accuracy. *Phys. Chem. Chem. Phys.* **2005**, *7*, 3297–3305.

(17) Frisch, M. J.; Trucks, G. W.; Schlegel, H. B.; Scuseria, G. E.; Robb, M. A.; Cheeseman, J. R.; Scalmani, G.; Barone, V.; Petersson, G. A.; Nakatsuji, H.; Li, X.; Caricato, M.; Marenich, A.; Bloino, J.; Janesko, B. G.; Gomperts, R.; Mennucci, B.; Hratchian, H. P.; Ortiz, J. V.; Izmaylov, A. F.; Sonnenberg, J. L.; Williams-Young, D.; Ding, F.; Lipparini, F.; Egidi, F.; Goings, J.; Peng, B.; Petrone, A.; Henderson, T.; Ranasinghe, D.; Zakrzewski, V. G.; Gao, J.; Rega, N.; Zheng, G.; Liang, W.; Hada, M.; Ehara, M.; Toyota, K.; Fukuda, R.; Hasegawa, J.; Ishida, M.; Nakajima, T.; Honda, Y.; Kitao, O.; Nakai, H.; Vreven, T.; Throssell, K.; Montgomery, J. A.; Peralta, J. E.; Ogliaro, F.; Bearpark, M.; Heyd, J. J.; Brothers, E.; Kudin, K. N.; Staroverov, V. N.; Keith, T.; Kobayashi, R.; Normand, J.; Raghavachari, K.; Rendell, A.; Burant, J. C.; Iyengar, S. S.; Tomasi, J.; Cossi, M.; Millam, J. M.; Klene, M.; Adamo, C.; Cammi, R.; Ochterski, J. W.; Martin, R. L.; Morokuma, K.; Farkas, O.; Foresman, J. B.; Fox, D. J.; *Gaussian 09*, Revision A.02, Gaussian, Inc.: Wallingford, CT, 2016.

(18) The electrostatic potential and the NBO charges of **int-3** were opposite with respect to **int-2**, where the tropone returns to a neutral state (−0.09 au), and the negative charge is mainly located on the alkoxide framework (−0.53 au).

(19) (a) Kumar, P.; Thakur, A.; Hong, X.; Houk, K. N.; Louie, J. Ni(NHC)]-Catalyzed Cycloaddition of Diynes and Tropone: Apparent Enone Cycloaddition Involving an 8π Insertion. *J. Am. Chem. Soc.* **2014**, *136*, 17844–17851. (b) Yang, X.-X.; Yan, R.-J.; Ran, G.-Y.; Chen, C.; Yue, J.-F.; Yan, X.; Ouyang, Q.; Du, W.; Chen, Y.-C. π -Lewis-Base-Catalyzed Asymmetric Vinylogous Umpolung Reactions of Cyclopentadienones and Tropone. *Angew. Chem., Int. Ed.* **2021**, *60*, 26762–26768.

(20) (a) Diccianni, J. B.; Diao, T. Mechanisms of Nickel-Catalyzed Cross-Coupling Reactions. *Trends Chem.* **2019**, *1*, 830–844. (b) Dawson, G. A.; Spielvogel, E. H.; Diao, T. Nickel-Catalyzed Radical Mechanisms: Informing Cross-Coupling for Synthesizing Non-Canonical Biomolecules. *Acc. Chem. Res.* **2023**, *56*, 3640–3653. (c) Day, C. S.; Martin, R. Comproportionation and Disproportionation in Nickel and Copper Complexes. *Chem. Soc. Rev.* **2023**, *52*, 6601–6616. (d) Day, C. S.; Rentería-Gómez, A.; Ton, S. J.; Gogoi, A. R.; Gutierrez, O.; Martin, R. Elucidating Electron-transfer Events in Polypyridine Nickel Complexes for Reductive Coupling Reactions. *Nat. Catal.* **2023**, *6*, 244–253.

(21) (a) Cerveri, A.; Giovanelli, R.; Sella, D.; Pedrazzani, R.; Monari, M.; Nieto Faza, O.; López, C. S.; Bandini, M. Enantioselective CO₂ Fixation via a Heck-Coupling/Carboxylation Cascade Catalyzed by Nickel. *Chem.—Eur. J.* **2021**, *27*, 7657–7662. (b) Lombardi, L.; Cerveri, A.; Giovanelli, R.; Castiñeira Reis, M.; Silva López, C.; Bertuzzi, G.; Bandini, M. Direct Synthesis of α -Aryl- α -Trifluoromethyl Alcohols via Nickel Catalyzed Cross-Electrophile Coupling. *Angew. Chem., Int. Ed.* **2022**, *134*, No. e202211732. (c) Lombardi, L.; Cerveri, A.; Cecon, L.; Pedrazzani, R.; Monari, M.; Bertuzzi, G.; Bandini, M. Merging C–C σ -bond Activation of Cyclobutanones with CO₂ Fixation via Ni-catalysis. *Chem. Commun.* **2022**, *58*, 4071–4074. (d) Giovanelli, R.; Lombardi, L.; Pedrazzani, R.; Monari, M.; Reis, M. C.; López, C. S.; Bertuzzi, G.; Bandini, M. Nickel Catalyzed Carbonylation/Carboxylation Sequence via Double CO₂ Incorporation. *Org. Lett.* **2023**, *25*, 6969–6974. (e) Giovanelli, R.; Monda, G.; Kiriakidi, S.; Silva López, C.; Bertuzzi, G.; Bandini, M. Direct Access to Benzolactams and Benzolactones via Nickel Catalyzed Carbonylation with CO₂. *Chem.—Eur. J.* **2024**, *30*, No. e202401658.

(22) Regarding the role of Zn-ions in sacrificial anode-based electrochemical processes see: (a) Su, Z.-M.; Deng, R.; Stahl, S. S. Zinc and Manganese Redox Potentials in Organic Solvents and their Influence on Nickel-catalysed Cross-electrophile Coupling. *Nat. Chem.* **2024**, *16*, 2036–2043. (b) Cardinale, L.; Beutner, G. L.; Bemis, C. Y.; Weix, D. J.; Stahl, S. S. Non-Innocent Role of Sacrificial Anodes in Electrochemical Nickel-Catalyzed C(sp²)–C(sp³) Cross-Electrophile Coupling. *J. Am. Chem. Soc.* **2024**, *146*, 32249–32254.

(23) Marcus, R. A.; Sutin, N. Electron Transfer in Chemistry and Biology. *Biochim. Biophys. Acta* **1985**, *811*, 265–322.

(24) Alcaide, B.; Almendros, P.; Aparicio, B.; Lázaro–Milla, C.; Luna, A.; Faza, O. N. Gold-Photoredox-Cocatalyzed Tandem Oxycyclization/Coupling Sequence of Allenols and Diazonium Salts with Visible Light Mediation. *Adv. Synth. Catal.* **2017**, *359*, 2789–2800.